

Preparation of $\text{Bi}_{2-x}\text{Sb}_x\text{Te}_3$ thermoelectric films by electrodeposition

Qinghua Huang, Wei Wang, Falong Jia, and Zhirong Zhang

Department of Applied Chemistry, School of Chemical Engineering and Technology, Tianjin University, Tianjin 300072, China

(Received 2005-04-11)

Abstract: $\text{Bi}_{2-x}\text{Sb}_x\text{Te}_3$ thermoelectric films were electrochemically deposited from the solution containing Bi^{3+} , HTeO_2^+ and SbO^+ . ESEM (environmental scanning electron microscope) investigations indicated that the crystalline state of $\text{Bi}_{2-x}\text{Sb}_x\text{Te}_3$ films transformed from equiaxed crystal to dendritic crystal with the negative shift of deposition potential. XRD and EDS were used to characterize the structure and composition of the electrodeposited films. The Seebeck coefficient and the temperature dependence of the resistance of $\text{Bi}_{2-x}\text{Sb}_x\text{Te}_3$ films were measured. The results showed that the composition of the film electrodeposited at -0.5 V is $\text{Bi}_{0.5}\text{Sb}_{1.5}\text{Te}_3$ with the largest Seebeck coefficient of $213 \mu\text{V}\cdot\text{K}^{-1}$.

Key words: thermoelectric films; bismuth antimony telluride compounds; electrodeposition; Seebeck coefficient; morphology

[This work was financially supported by the National Key Project on Basic Research of China (No.ZM200103A01).]

1. Introduction

In the last decade, green power sources have attracted much attention because of severe environmental problem. As a green power source, the greatest virtue of a thermoelectric power generator is that it makes use of all kinds of heat (solar heat, ocean heat, geothermal heat, waste heat, body heat, *etc.*) to transform them to electric power with great efficiency. It has a long working life (over 20 years) in a wide temperature range with highly stable performance. The power generation efficiency mainly depends on the performance of thermoelectric materials, which can be typically expressed by the dimensionless quantity ZT , where T is the temperature and Z is the thermoelectric figure of merit. $ZT = T\alpha^2\sigma/\lambda$, where α is the Seebeck coefficient, σ is the electrical conductivity, and λ is the thermal conductivity. Many studies [1-6] have been done to improve ZT value of the thermoelectric materials in recent years.

Bismuth and antimony telluride-based materials are of great interest for thermoelectric applications in the temperature range of 200-400 K. In general, the thermoelectric films of bismuth and antimony telluride-based materials are fabricated by chemical or physical vapor deposition [7-8]. Compared to these techniques, the electrodeposition may offer a simple and low cost growth method for thermoelectric materials. The most advantageous point of the electrodeposition is that the

doping concentration and crystalline state of thermoelectric films can be easily controlled through adjusting the parameters of electrodeposition. M.G. Marisol *et al.* [9] first reported the fabrication of high-density Sb-rich $\text{Bi}_{2-x}\text{Sb}_x\text{Te}_3$ nanowire arrays by means of the electrodeposition technique. However, the thermoelectric performance of the electrodeposited $\text{Bi}_{2-x}\text{Sb}_x\text{Te}_3$ has not been yet examined. In this study, the electrodeposition technology was used to prepare a $\text{Bi}_{2-x}\text{Sb}_x\text{Te}_3$ thermoelectric film. The morphology, structure, composition and the relation between the Seebeck coefficient and the electrodeposition parameters of the film were reported here.

2. Experimental

The $\text{Bi}_{2-x}\text{Sb}_x\text{Te}_3$ thermoelectric films were prepared by potentiostatic electrodeposition in a three-electrode cell consisting of a Cu plate as the working electrode, a Pt plate as the auxiliary electrode and a saturated calomel electrode (SCE) as the reference electrode. The cyclic voltammetric curves were measured using CHI660B electrochemical station at room temperature. All the processes were carried out under an inert atmosphere (nitrogen) condition.

The electrolytes were prepared with redistilled water to ensure the stability of ions in the solution. The Bi and Te solution was prepared by dissolution of $\text{Bi}(\text{NO}_3)_3$ and H_2TeO_3 in 1 mol/L aqueous HNO_3 . The

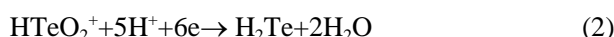
Sb solution was obtained by dissolution of Sb_2O_3 in complexing agents such as citric acid, tartaric acid or EDTA, to get high concentration because of low solubility of Sb salts. The Bi^{3+} , HTeO_2^+ and SbO^+ electrolyte mixtures were obtained from the above solutions.

The morphology of the $\text{Bi}_{2-x}\text{Sb}_x\text{Te}_3$ thermoelectric films was analyzed using PHILIPS XL30 environmental scanning electron microscope (ESEM). The composition of the film was assessed by D/MAX-2500 XRD and EDS in ESEM. The Seebeck coefficient and resistance of the thermoelectric films were measured by the thermoelectric performance measurement system developed by Tianjin University.

3. Results and discussion

Fig. 1(a) shows the cyclic voltammogram of the Bi^{3+} , HTeO_2^+ and SbO^+ electrolyte. During a cathodic process, the curve obtained shows two reduction waves A and B. In comparison with Fig. 1(a), the reduction process for the Bi^{3+} and SbO^+ electrolyte without HTeO_2^+ is shown in Fig. 1(b). It can be found that there is one reduction wave D in the Bi^{3+} and SbO^+ electrolyte without HTeO_2^+ . The results imply that HTeO_2^+

plays an important role in the reduction process. Previous studies have shown that HTeO_2^+ adsorbs strongly onto Pt electrodes [10]. For this reason, the following reaction sequence has been proposed on the formation of $\text{Bi}_{2-x}\text{Sb}_x\text{Te}_3$ from the Bi^{3+} , HTeO_2^+ and SbO^+ electrolyte [9]. Peak A at -0.09 V presents the reduction of HTeO_2^+ to Te, followed by the reduction of HTeO_2^+ to H_2Te for the peak B at -0.18 V. The potential region is different from the value reported by M.G. Marisol *et al.* [9]. The main reason for this disagreement could be the difference of ionic concentrations and additives. The reactions for the peaks A and B in the nitric acid solution can be presented as:



After this electrochemical reduction, Bi^{3+} and SbO^+ in the solution react with Te or H_2Te to produce $\text{Bi}_{2-x}\text{Sb}_x\text{Te}_3$. The overall reaction can be expressed as follows:

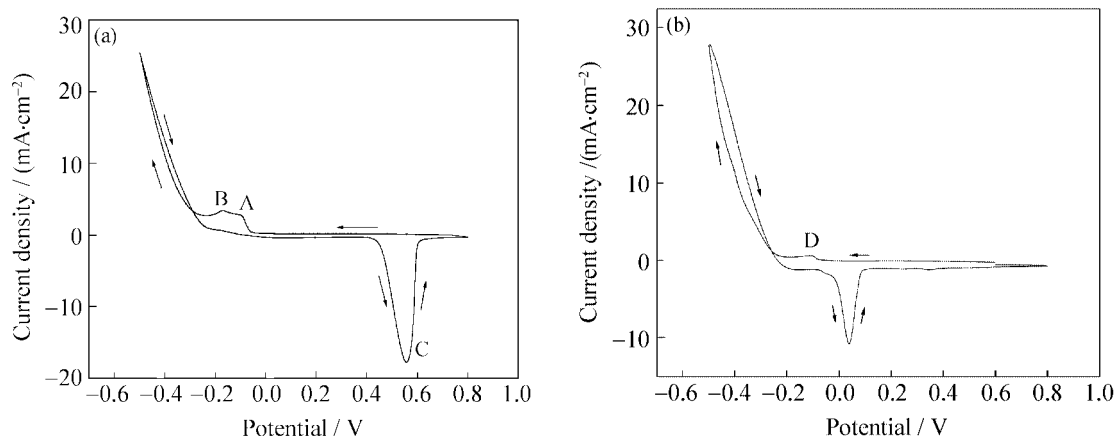
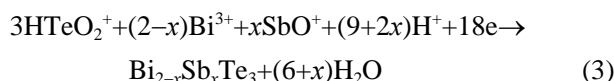


Fig. 1. Cyclic voltammograms of (a) Bi^{3+} (1.5 mmol/L), HTeO_2^+ (12.4 mmol/L), SbO^+ (7.2 mmol/L), tartaric acid (0.65 mol/L) in HNO_3 (1 mol/L) and (b) Bi^{3+} (1.5 mmol/L), SbO^+ (7.2 mmol/L), tartaric acid (0.65 mol/L) in HNO_3 (1 mol/L). Scan rate= 100 $\text{mV}\cdot\text{s}^{-1}$, Pt electrode.

In the reverse sweep, there is only one wave at 0.55 V for the oxidation of the deposit. It indicates that only $\text{Bi}_{2-x}\text{Sb}_x\text{Te}_3$ can be obtained during the cathodic process in the solution containing Bi^{3+} , SbO^+ and HTeO_2^+ . As will be discussed below, the formation of $\text{Bi}_{2-x}\text{Sb}_x\text{Te}_3$ as opposed to the deposition of Bi, Te and Sb layers is confirmed by XRD, as all the diffraction maxima can be indexed with a single phase for the film.

According to Fig. 1, $\text{Bi}_{2-x}\text{Sb}_x\text{Te}_3$ films were electro-deposited by controlling different potentials in the region from -0.1 to -0.6 V. The thickness of the films was estimated from the total electric charge passed

through the working electrode assuming the current efficiency of 100%.

$$\delta = QM/AdFz \quad (4)$$

where δ is the thickness of the film, Q is the total electric charge, M is the formula weight of $\text{Bi}_{2-x}\text{Sb}_x\text{Te}_3$, A is the area of the working electrode, d is the density of $\text{Bi}_{2-x}\text{Sb}_x\text{Te}_3$, z is the charge number ($z=18$) and F is the Faraday constant. To keep the same thickness of $\text{Bi}_{2-x}\text{Sb}_x\text{Te}_3$ films prepared at different potentials, the total electric charge was fixed at 18 C. The film with $d=10$ μm was obtained under this condition.

ESEM images of the $\text{Bi}_{2-x}\text{Sb}_x\text{Te}_3$ films electrodeposited at different potentials are shown in Fig. 2. It can be found that the surface of the $\text{Bi}_{2-x}\text{Sb}_x\text{Te}_3$ film electrodeposited at -0.1V is dense and uniform with an average crystallite size of $2\ \mu\text{m}$, while the surface of the

film prepared at -0.3V or -0.5V is rough with dendritic growth. The results demonstrate that the crystalline state of the $\text{Bi}_{2-x}\text{Sb}_x\text{Te}_3$ film transforms from equiaxed crystal to dendritic crystal with the negative shift of deposition potential.

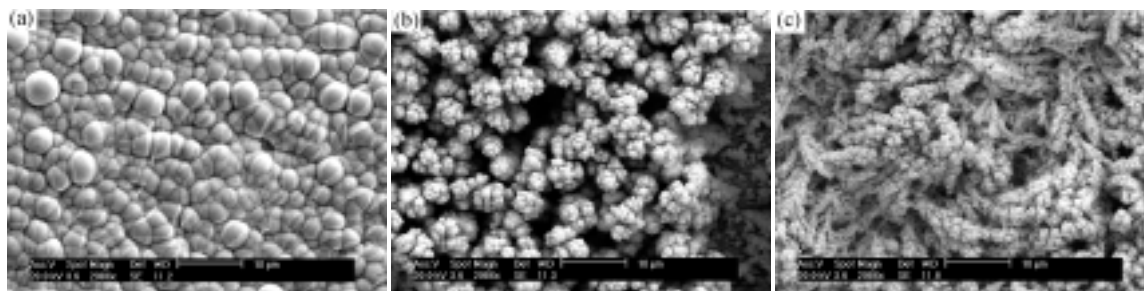


Fig. 2. ESEM images of the $\text{Bi}_{2-x}\text{Sb}_x\text{Te}_3$ films electrodeposited at different potentials: (a) -0.1V ; (b) -0.3V ; (c) -0.5V .

The XRD pattern of the film electrodeposited at -0.5V are shown in Fig. 3. The diffraction peaks are found to be consistent with the standard pattern of $\text{Bi}_{0.5}\text{Sb}_{1.5}\text{Te}_3$ (JCPDS49-1713). Further analysis indicates that the peak intensity of crystal plan (110) increases while the peak intensity of crystal plan (1010) decreases. It appears that the crystal orientation of the electrodeposited film prefers to crystal plan (110). EDS analysis proves that the composition of the film is $\text{Bi}_{0.5}\text{Sb}_{1.4}\text{Te}_{3.1}$ (shown in Fig. 4), which is very close to the perfect composition of $\text{Bi}_{0.5}\text{Sb}_{1.5}\text{Te}_3$. Based on the results of XRD and EDS analyses, it can be concluded that the thermoelectric film electrodeposited at -0.5V is single phase with the composition of $\text{Bi}_{0.5}\text{Sb}_{1.5}\text{Te}_3$.

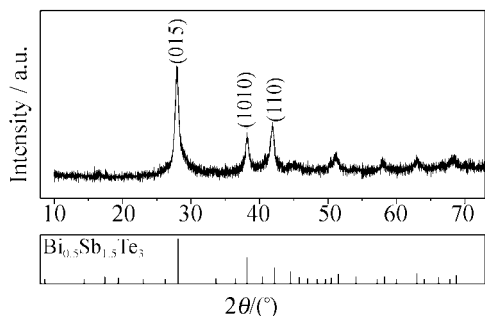


Fig. 3. XRD pattern of the electrodeposited film at -0.5V .

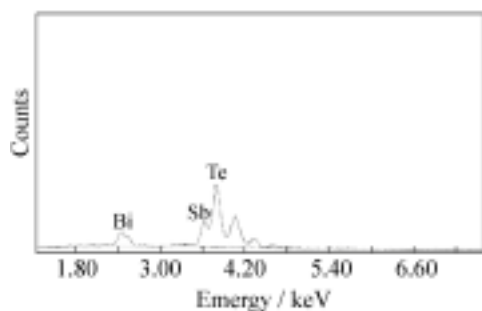


Fig. 4. EDS pattern of the electrodeposited film at -0.5V .

The resistance of the $\text{Bi}_{2-x}\text{Sb}_x\text{Te}_3$ film electrode-

posited at -0.5V was measured using a Keithly 2000 multimeter in the temperature range from 297 to 319 K. The results are reported in Fig. 5. The resistance decreases slightly with temperature, from 0.159 to $0.069\ \Omega$, which indicates a semiconductive nature.

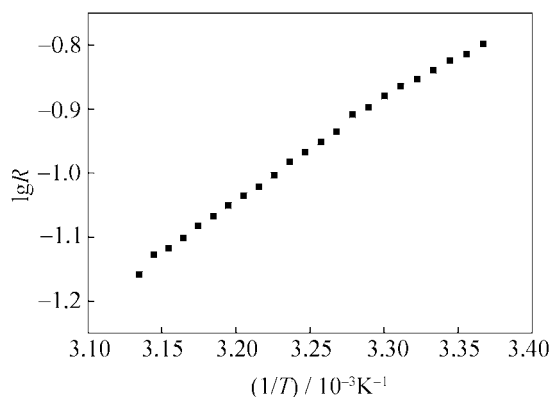


Fig. 5. Temperature dependence of the film electrodeposited at -0.5V .

The Seebeck coefficient measurement at room temperature was performed on the $\text{Bi}_{2-x}\text{Sb}_x\text{Te}_3$ films electrodeposited at different potentials. It can be seen in Fig. 6 that the semiconductive type of the films is p-type.

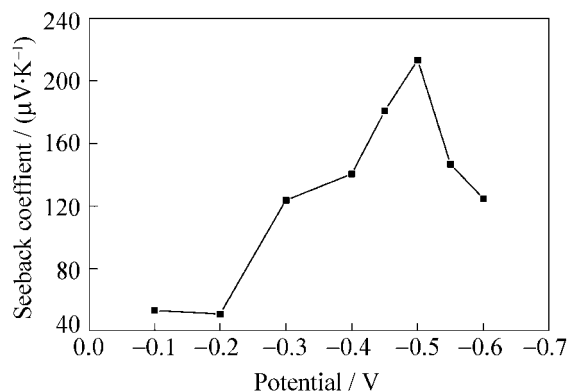


Fig. 6. Relation between the Seebeck coefficient of $\text{Bi}_{2-x}\text{Sb}_x\text{Te}_3$ films and depositing potential.

The value of the Seebeck coefficient increases with the negative shift of the electrodeposition potential and reaches the largest Seebeck coefficient of about $213 \mu\text{V}\cdot\text{K}^{-1}$ at -0.5 V . After that the Seebeck coefficient decreases with the negative shift of the potential. The results show that the doping concentration of $\text{Bi}_{2-x}\text{Sb}_x\text{Te}_3$ thermoelectric films can be controlled by adjusting the electrodeposition potential, and their thermoelectric properties can also be controlled.

4. Conclusions

$\text{Bi}_{2-x}\text{Sb}_x\text{Te}_3$ films were fabricated by the electrodeposition using nitric acid solution containing Bi^{3+} , SbO^+ and HTeO_2^+ . ESEM studies indicated that the crystalline state of the $\text{Bi}_{2-x}\text{Sb}_x\text{Te}_3$ films transforms from equiaxed crystal to dendritic crystal with the negative shift of electrodeposition potential. XRD and EDS results revealed that the thermoelectric film electrodeposited at -0.5 V is single phase with $\text{Bi}_{0.5}\text{Sb}_{1.5}\text{Te}_3$ composition. Thermoelectric performance measurement of the $\text{Bi}_{2-x}\text{Sb}_x\text{Te}_3$ films electrodeposited at different potentials showed that the conductive type of the films is p-type and its doping concentration can be controlled through adjusting electrodeposition potential, and their thermoelectric properties can also be controlled. The film electrodeposited at -0.5 V possesses the largest Seebeck coefficient of $213 \mu\text{V}\cdot\text{K}^{-1}$. With the increase of temperature, the resistance of the electrodeposited $\text{Bi}_{0.5}\text{Sb}_{1.5}\text{Te}_3$ film is reduced and shows a semiconductive characteristic.

References

- [1] W. Wang, Q.H. Huang, F.L. Jia, *et al.*, Electrochemically assembled P-type Bi_2Te_3 nanowire arrays, *J. Appl. Phys.*, 96(2004), No.1, p.615.
- [2] M.S. Sander, R. Gronsky, T. Sands, *et al.*, Structure of bismuth telluride nanowire arrays fabricated by electrodeposition into porous anodic alumina templates, *Chem. Mater.*, 15(2003), No.1, p.335.
- [3] L.D. Hicks, T.C. Harman, and M.S. Dresselhaus, Use of quantum-well superlattices to obtain a high figure of merit from nonconventional thermoelectric materials, *Appl. Phys. Lett.*, 63(1993), No.23, p.3230.
- [4] B.C. Sales, D. Mandrus, and R.K. Williams, A filled skutterudite antimonides: a new class of thermoelectric materials, *Science*, 272(1996), No.5266, p.1325.
- [5] Y. Miyazaki and T. Kajitani, Preparation of Bi_2Te_3 films by electrodeposition, *J. Crystal Growth*, 229(2001), No.4, p.542.
- [6] X.B. Zhao, S.H. Hu, M.J. Zhao, *et al.*, Thermoelectric properties of $\text{Bi}_{0.5}\text{Sb}_{1.5}\text{Te}_3$ /polyaniline hybrids prepared by mechanical blending, *Mater. Lett.*, 52(2002), No.3, p.147.
- [7] R. Venkatasubramanian, T. Colpitts, E. Watko, *et al.*, MOCVD of Bi_2Te_3 , Sb_2Te_3 and their superlattice structures for thin-film thermoelectric applications, *J. Crystal Growth*, 170(1997), No.4, p.817.
- [8] B. Aboulfarah, A. Mzerd, A. Giani, *et al.*, Elaboration of $(\text{Bi}_{1-x}\text{Sb}_x)_2\text{Te}_3$ thin films by metallorganic chemical vapor deposition, *J. Mater. Sci. Lett.*, 18(1999), No.13, p.1095.
- [9] M.G. Marisol, L.P. Amy, G. Ronald, *et al.*, High-density 40 nm diameter Sb-rich $\text{Bi}_{2-x}\text{Sb}_x\text{Te}_3$ nanowire arrays, *Adv. Mater.*, 15(2003), No.12, p.1003.
- [10] T. Montiel-Santillán, O. Solorza, and H. Sánchez, Electrochemical research on tellurium deposition from acid sulfate medium, *J. Solid State Electrochem.*, 6(2002), No.7, p.433.